PHYSICAL REVIEW D VOLUME 3, NUMBER 7 1 APRIL 1971

Quark Model of Diffractive Processes*

J. S. BALL
Department of Physics, University of Utah, Salt Lake City, Utah 84112

AND

F. ZACHARIASEN
Department of Physics, California Institute of Technology, Pasadena, California 91109
(Received 14 December 1970)

Numerical results from a previously described model of diffraction scattering with nonshrinking forward peaks are presented, and the model is reformulated in terms of quarks with a view to making it more realistic.

I. INTRODUCTION

In an earlier paper[1] we described a model of high-energy diffraction scattering based on the assumption that the asymptotic form of the scattering amplitude is $isf(t)$. We also obtained from the model an integral equation for $f(t)$, the shape of the diffraction peak.

We should like, here, to report on approximate solutions to this integral equation obtained numerically on a computer. The results obtained have a number of features in common with experimentally observed diffraction peaks, and they seem sufficiently encouraging to warrant pursuing the model further.

There were some oversimplifications in the original version of the model, the most serious of which was that the model was phrased in terms of only a single kind of particle (a "parton"?). We calculated cross sections, multiplicities, and so forth, only for this "particle" and made no attempt to predict from the behavior of these what the corresponding quantities for the spectrum of physically observable particles should be. There are really only two things with which this particle could be identified. It could be just any one of the existing spectrum of strongly interacting particles, or it could be a quark. In the first case, it must be assumed that at very high energies, all strongly interacting particles behave in the same way. In particular, all elastic scattering amplitudes should become equal; and indeed this is not too far from what is observed even at present energies. There is a difficulty with this interpretation, however, and it is that the average multiplicity predicted by the model for the basic particle is, asymptotically, constant. If our particle is itself any hadron, this prediction seems to be at variance with experiment.[2] Thus the model might be, at best, only approximately true in some limited energy range.

If, however, the second interpretation of our parton obtains and it is in fact a quark, then there is no difficulty with the multiplicity. It is only the quark multiplicity that is predicted to be a constant, not the multiplicity of observed hadrons. If the quark multiplicity is constant, then $q\bar{q}$ states will be produced with a mass which increases as the total energy of the reaction increases. States of $q\bar{q}$ with high mass also have high spin, so they will decay into hadrons. How many hadrons they decay into depends on quark dynamics and cannot therefore be predicted cleanly; nevertheless, one may expect that the higher the $q\bar{q}$ spin, the larger the number of stable hadrons which will finally be produced. Thus the multiplicity of observed hadrons will grow, albeit in a way we cannot easily predict, if our particle is identified with a quark.

One further remark is worth making at this point. Whatever the interpretation of our particle, the model we have is *not* a model of the multiperipheral or multi-Regge[3] type, although it has certain similarities to these. Our model is mathematically equivalent to what one would obtain from a multi-Regge model with multiple exchange of a flat Pomeranchon having a trajectory of $\alpha_P=1$, and for which the internal coupling constant vanishes like $(\log s)^{-1/2}$. However, in a true multi-Regge theory the internal vertices cannot depend on the total energy, but only on the two adjacent momentum transfers and a Toller angle ω.[4] If one feels compelled to identify our model with some sort of diagram structure, the simplest diagram which might have the behavior we propose is that shown in Fig. 1.

II. SOLUTION TO INTEGRAL EQUATION

Let us first consider the possibility that our particle is any hadron. Then, as in the original version of the model,[1] the integral equation obtained from the require-

* Work supported in part by the U. S. Atomic Energy Commission.

[1] J. S. Ball and F. Zachariasen, Phys. Letters **30B**, 558 (1969).

[2] Experiment seems to show at least a logarithmic increase of n with s. See L. Jones, in Proceedings of International Conference on Expectations for Particle Reactions, University of Wisconsin (unpublished).

[3] K. ter-Martirosyan, Zh. Eksperim. i Teor. Fiz. **44**, 341 (1963) [Soviet Phys. JETP **17**, 233 (1963)]; T. W. B. Kibble, Phys. Rev. **131**, 2282 (1963); Chan Hong-Mo, K. Kajantie, and G. Ranft, Nuovo Cimento **49**, 157 (1967); F. Zachariasen and G. Zweig, Phys. Rev. **160**, 1326 (1967).

[4] H. M. Chan, K. Kajantie, and G. Ranft, Nuovo Cimento **49**, 157 (1967); N. F. Bali, G. F. Chew, and A. Pignotti, Phys. Rev. **163**, 1572 (1967).

ment of s-channel unitarity for $f(t)$ is

$$f(t)=g(t)e^{Cg(t)}, \tag{2.1}$$

where

$$g(t)=\frac{1}{16\pi^2}\int\int\frac{f(t_1)f(t_2)dt_1dt_2}{(2tt_1+2tt_2+2t_1t_2-t^2-t_1{}^2-t^2)^{1/2}}. \tag{2.2}$$

The range of integration in Eq. (2.2) is over all t_1 and t_2 such that the argument of the square root is positive.

The constant C is a parameter. The normalization is such that $f(0)=\sigma_T$, the total cross section, and $g(0)=\sigma_e$, the elastic cross section. Thus

$$Cg(0)=\ln(\sigma_T/\sigma_e). \tag{2.3}$$

The differential cross section is given by

$$\frac{d\sigma}{dt}=\frac{1}{16\pi}|f(t)|^2. \tag{2.4}$$

To study possible analytic solutions to Eqs. (2.1) and (2.2), let us first redefine g and f by dividing by 8π. The resulting equations are

$$g(t)=\frac{1}{2\pi}\int dt_1dt_2f(t_1)f(t_2)\times\frac{1}{(2t_1t+2t_1t_2+2tt_2-t^2-t_1{}^2-t_2{}^2)^{1/2}}, \tag{2.5a}$$

$$f(t)=g(t)e^{C'g(t)}, \tag{2.5b}$$

where C' is $8\pi C$. We now expand both g and f in a power series in C' and identify coefficients:

$$g=\sum_{i=0}^{\infty}g_i(C')^i,\qquad f=\sum_{i=0}^{\infty}f_i(C')^i. \tag{2.6}$$

The first few equations are as follows:

$$f_0=g_0,\quad f_1=g_0{}^2+g_1,\quad f_2=\tfrac{1}{2}g_0{}^3+2g_0g_1+g_2, \tag{2.7}$$

and, in general,

$$f_n=P_n(g_0,\ldots,g_{n-1})+g_n,$$

where P_n is a known polynomial function of its arguments. The Bessel transform of a function is

$$G(b)=\int_0^{\infty}(-t)^{1/2}d(-t)^{1/2}J_0((-t)^{1/2}b)g(-t)^{1/2}, \tag{2.8}$$

and will be denoted

$$G(b)=\text{B.T.}[g].$$

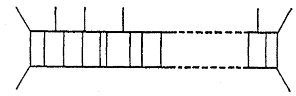

FIG. 1. Class of Feynman diagrams for production which the model may be describing.

Note that

$$\text{B.T.}(GH)=\frac{1}{2\pi}\int dt_1\int dt_2g(\sqrt{t_1})h(\sqrt{t_2})\times(2tt_1+2t_1t_2+2tt_2-t_1{}^2-t_2{}^2-t^2)^{-1/2}. \tag{2.8'}$$

Therefore, the Bessel transform of Eq. (2.5a) is simply

$$G=F^2. \tag{2.9}$$

If we then write the Bessel transforms of Eq. (2.7), the first one becomes

$$F_0=F_0{}^2, \tag{2.10}$$

and hence any function that is either zero or one for positive b is a solution. In particular, if F_0 is a step function $\theta(R-b)$, then

$$f_0(t)=\frac{J_1((-t)^{1/2}R)}{(-t)^{1/2}}R, \tag{2.11}$$

which is a typical form used to fit diffraction phenomena. For any particular F_0 we can now, by quadrature, generate the higher-power terms as follows. From Eq. (2.5a),

$$G_n=2F_0F_n+\sum_{i=1}^{n-1}F_iF_{n-i}, \tag{2.12}$$

and from Eq. (2.7),

$$F_n=\text{B.T.}(P_n)+G_n,\qquad F_n=[\text{B.T.}(P_n)+\sum_{i=1}^{n-1}F_iF_{n-i}](1-2F_0), \tag{2.13}$$

where we have used the fact that $(1-2F_0)$ is ±1. Thus for sufficiently small C', we obtain a solution for each possible F_0, and there are therefore infinitely many solutions to our system of equations.

In practice the difficulties in performing repeated Bessel transforms numerically make the above method of solution impractical and, furthermore, the series may not converge at all for the rather large value of C' ($C'\approx2$) that seems to be indicated by experiment. To attempt to find a solution numerically, we will simply guess a function $f(t)$, and if it nearly reproduces itself through Eqs. (2.1) and (2.2), we shall then accept it as an approximate solution.

We chose to try a four-parameter form of $g(t)$:

$$g(t)=\frac{g(0)}{(1-t/t_0)^n}\left[1+\frac{at}{(1-t/t_0)^2}\right]. \tag{2.14}$$

A value of $f(0)$ was imposed (and taken to be 112

TABLE I. Approximate solution for pp. The columns labeled f are the f of Eq. (2.1) divided by the experimental value at $t=0$. The subscripts 0, 1, 2, refer to the input, first, and second iteration, respectively, of Eqs. (2.2) and (2.1).

$-t$ in GeV^2	$f_0(t)$	$f_1(t)$	$g(t)_0$	$g(t)_1$	$g(t)_2$
0.00	1.00	1.05	16.5	16.8	17.1
0.14	0.34	0.34	10.9	10.8	10.9
0.23	0.207	0.205	8.6	8.6	8.7
0.36	0.114	0.115	6.22	6.27	6.16
0.55	0.058	0.059	4.08	4.13	4.26
0.82	0.028	0.029	2.38	2.48	2.39
1.22	1.28×10^{-2}	1.39×10^{-2}	1.24	1.33	1.34
1.83	5.5×10^{-3}	6.1×10^{-3}	0.58	0.63	0.63
2.78	2.2×10^{-3}	2.5×10^{-3}	0.239	0.267	0.265
4.31	7.6×10^{-4}	8.6×10^{-4}	0.84	0.096	0.098
6.95	2.1×10^{-4}	2.5×10^{-4}	2.3×10^{-2}	2.8×10^{-2}	3.0×10^{-2}
11.9	4.0×10^{-5}	5.3×10^{-5}	4.4×10^{-3}	5.9×10^{-3}	6.5×10^{-3}
22.2	4.5×10^{-6}	7.4×10^{-6}	5.1×10^{-4}	8.3×10^{-4}	1.1×10^{-3}

GeV^{-4} in conformity with the experimental value of the proton-proton total cross section; this number sets the dimensional scale) determining C for each value of $g(0)$ used. Then a computer search among the four numbers $g(0)$, n, t_0, and a was made to find the optimal values for which the input and once-iterated solutions best agreed.[5] The best-fit input-output values of $f(t)$, together with the results of a second iteration, are shown in Table I; we see that the input and output differ by less than 30% over 14 decades in size. The agreement between the first and second iterations is remarkably good. However, numerical inaccuracy makes additional iterations unreliable. The best values of the four parameters are $n=4.1$, $t_0=2.0$, $g(0)=16.55$, and $a=1.0$, so that $\sigma_T/\sigma_e=6.77$. For proton-proton scattering, the experimental value of σ_T/σ_e is 4.1 at 19.6 GeV.

For large t, that is, if $|t|\gg t_0$, then the solution looks like a power:

$$f(t)\approx g(t)\approx g_0\left(\frac{t_0}{|t|}\right)^n. \tag{2.15}$$

It is interesting to note that our optimum value of n was 4.1. A popular theory of large-t proton-proton scattering states that $f(t)$ should be proportional to the square of the electromagnetic form factor of the proton[6]:

$$f(t)/f(0)=|F(t)|^2. \tag{2.16}$$

This, since $F(t)\sim t^{-2}$, would say $f(t)$ goes like t^{-4} for large t.

Our solution for $f(t)/f(0)$, together with experimental values[7] and $|F(t)|^2$, is shown in Fig. 2.

Altogether, with only one input parameter [the value of $f(0)$], remarkable similarity exists between our solution and experiment; thus we are encouraged to pursue the model further.

III. EXTENSION TO QUARK MODEL

Let us rephrase the model in terms of quarks. There are three kinds of quarks with two spin states each; let us label these by indices α, β, $\cdots$, etc., ranging from 1 to 6. Let us assume that the elastic scattering amplitude for a quark α or a quark β is of the $isf(t)$ form, and let us assume that it factors. Thus we write, at large s and fixed t,

$$T_{\alpha\beta\to\alpha\beta}(s,t)\to is[f_\alpha(t)f_\beta(t)]^{1/2}. \tag{3.1}$$

A representation of this process is shown in Fig. 3(a). We may think of $[f_\alpha(t)]^{1/2}$ as the coupling of a flat Pomeranchon to the quark α.

It should be noted that a factorized form of this sort could lead to difficulties in the description of scattering from large composite systems. This is the same difficulty remarked on originally with regard to the factorization of Regge residues and the applicability of Regge theory to heavy nuclei.[8] The difficulty is that if the scattering of a quark from an individual quark is as

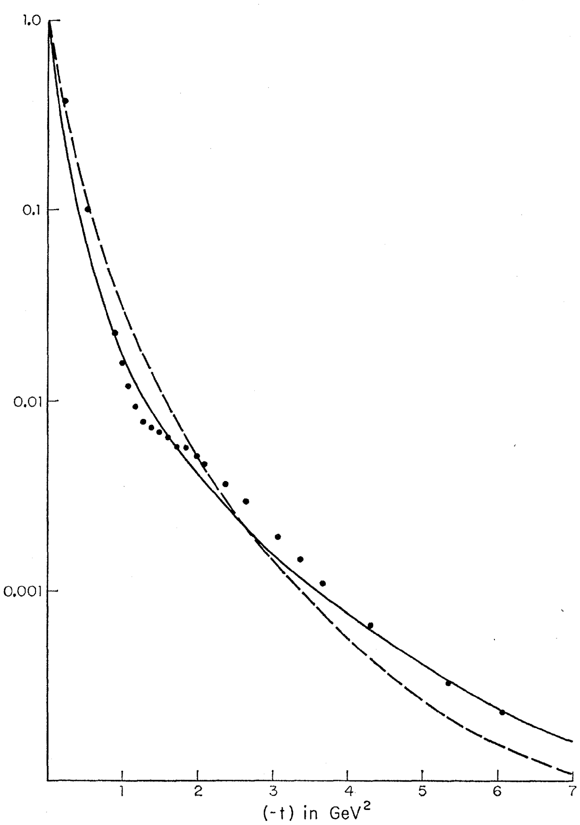

FIG. 2. Calculated value of $f(t)/f(0)$ for pp is the solid curve. The dashed curve is $|F(t)|^2$ and the data points are for pp scattering at 19.6 GeV, from Ref. 7.

[5] The equation is unstable with respect to perturbations of the over-all scale of g, unfortunately, so repeated iterations of the approximate solution lead rapidly to chaos.

[6] T. T. Chou and C. N. Yang, Phys. Rev. **170**, 1591 (1968); H. D. I. Abarbanel, S. D. Drell, and F. J. Gilman, Phys. Rev. Letters **20**, 280 (1968).

[7] J. V. Allaby *et al.*, Phys. Letters **38B**, 67 (1968).

[8] M. Gell-Mann and B. M. Udgaonkar, Phys. Rev. Letters **8**, 346 (1962).

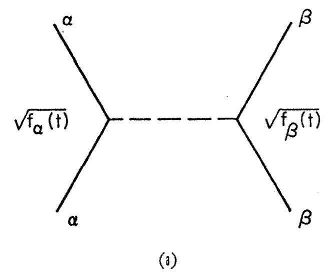

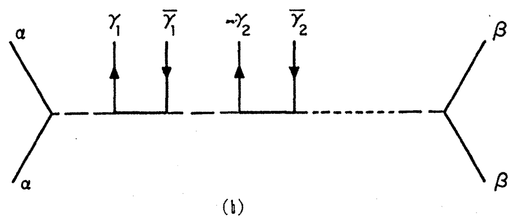

FIG. 3. (a) Diagram for quark-quark elastic scattering. (b) Diagram for the process $qq \to qq+N(q\bar{q})$.

given in Eq. (3.1), and if a large composite system is made up of N quarks, then one might say that the amplitude to scatter from the composite system is

$$[f_\alpha(t)]^{1/2} \sum_{\beta=1}^{N} [f_\beta(t)]^{1/2}.$$

This leads to the result that the total cross section for a quark on the large system is N times the quark-quark cross section for a quark on the large system is N times the quark-quark cross section. Yet experimentally total cross sections or nuclei grow like $A^{2/3}$ rather than A.

The resolution of the difficulty lies in the fact that multiple-scattering phenomena are important, so that for large composite objects the form assumed above for the amplitude is invalid. This point is returned to with an estimate of the importance of multiple scattering in Sec. IV.

Next, as in the simplified version of the model, let us represent the amplitude to produce N $q\bar{q}$ pairs of type $\gamma_1\bar{\gamma}_1\cdots\gamma_N\bar{\gamma}_N$ in the $\alpha\beta$ collision by

$$\begin{aligned} T_{\alpha\beta\to\alpha\beta\ \gamma_1\bar{\gamma}_1\ldots\gamma_N\bar{\gamma}_N} &= iF_{\gamma_1\ldots\gamma_N}(s)[f_\alpha(t_1)]^{1/2}[f_{\gamma_1}(t_1)]^{1/2} \\ &\quad\times P_{\gamma_1}(t_1')[f_{\gamma_1}(t_2)]^{1/2}[f_{\gamma_2}(t_2)]^{1/2} \\ &\quad\times P(t_2')\cdots[f_\beta(t_{n-1})]^{1/2}. \end{aligned} \quad (3.2)$$

The corresponding diagram and labeling is shown in Fig. 4(b). The quarks must be produced diffractively in pairs, so that $\bar{\gamma}_1$ stands for the antiquark of the quark γ_1. $P_\gamma(t)$ is a quark propagator between the two Pomeranchon couplings attached to the γ quark-antiquark pair. $F_{\gamma_1\ldots\gamma_N}(s)$ with $N=0$ is just s, in conformity with Eq. (3.1).

We continue to proceed as before; the next step is to impose s-channel multiparticle unitarity. This yields in complete analogy to Ref. 1 the equation

$$\begin{aligned} \mathrm{Im}T_{\alpha\beta\to\alpha\beta}(s,t) &= s\sum_{N=0}^{\infty}\sum_{\gamma_1\cdots\gamma_N=1}^{6}\left|\frac{F_{\gamma_1\ldots\gamma_N}(s)}{s}\right|^2 \\ &\quad\times g_{\alpha\gamma_1}(t)p_{\gamma_1}(t)g_{\gamma_1\gamma_2}(t)p_{\gamma_2}(t)\cdots p_{\gamma_N}(t)g_{\gamma_N\beta}(t) \\ &\quad\times\left[\frac{(1/\pi)\ln s}{2N!}\right]^{2N}, \end{aligned} \quad (3.3)$$

where

$$g_{\alpha\beta}(t)=\frac{1}{16\pi^2}\int\int\frac{dt_1dt_2}{(2tt_1+2tt_2+2t_1t_2-t^2-t_1^2-t_2^2)^{1/2}} \times[f_\alpha(t_1)]^{1/2}[f_\beta(t_1)]^{1/2}[f_\alpha(t_2)]^{1/2}[f_\beta(t_2)]^{1/2} \quad (3.4)$$

and

$$p_\gamma(t)=\frac{1}{16\pi^2}\int\int\frac{P_\gamma(t_1)P_\gamma(t_2)dt_1dt_2}{(2tt_1+2tt_2+2t_1t_2-t^2-t_1^2-t_2^2)^{1/2}}. \quad (3.5)$$

Thus g and p stand for the alternating boxes in Fig. 5. We may note that for large quark mass $p_\gamma(t)$ becomes a constant.

We shall now assume, as before, that the internal quark-Pomeranchon vertices vanish. We then choose

$$F_{\gamma_1\ldots\gamma_N}(s)=s(\pi C/\ln s)^N, \quad (3.6)$$

where C is some constant. This amounts to assuming that the partial cross sections σ_N to produce N $q\bar{q}$ pairs

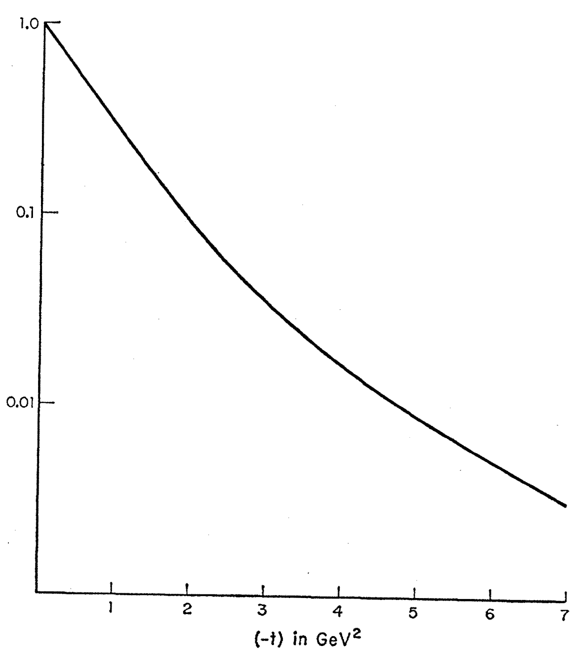

FIG. 4. Calculated value of $f(t)/f(0)$ for qq scattering.

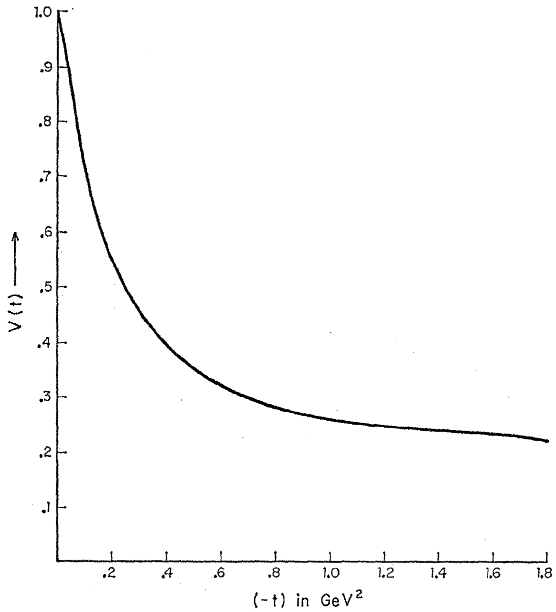

FIG. 5. Value of $V(t)$ obtained from the calculated values of $f(t)$ for pp and $f(t)$ for qq.

are Poisson distributed in N and constant in s for large s. Equation (3.3), when combined with Eq. (3.1), then becomes

$$[f_\alpha(t)]^{1/2}[f_\beta(t)]^{1/2} = g_{\alpha\beta}(t) + \frac{g_\alpha(t) g_\beta(t)}{g(t)}\{\cosh([Cp(t)g(t)]^{1/2}) - 1\}, \quad (3.7)$$

where we define

$$g_\alpha(t) = \sum_{\beta=1}^{6} g_{\alpha\beta}(t) \quad (3.8)$$

and

$$g(t) = \sum_{\alpha=1}^{6} g_\alpha(t). \quad (3.9)$$

At this point we shall simplify the model by assuming $SU(6)_W$ symmetry (thereby neglecting the indices) and by assuming $p(t)$ to be a constant. We then find

$$f(t) = g(t)\cosh([Cg(t)]^{1/2}). \quad (3.10)$$

This is very much the same as the corresponding equation of the original version of the model, namely, Eq. (2.1). The quark-quark or quark-antiquark total cross section is simply $f(0)$; the quark-quark (or quark-antiquark) differential cross section is $(1/16\pi)|f(t)|^2$. The function $g(t)$ is related to $f(t)$ by Eq. (2.2).

To obtain an approximate solution to Eq. (3.10), we employ the same method as for the original version of the model. However, $f(0)$ is now normalized to 12 GeV^{-4} in accordance with the expected 9:1 ratio of total cross sections. The trial function used was that given in Eq. (2.14). The results for the best values of the parameters are given in Table II. Again we are able to obtain a function that reproduces itself rather well and is quite stable under an additional iteration. The values of the parameters in this case were $g(0)=1.15$, $n=4.5$, $t_0=5.0$, and $a=-0.5$. As before, no appreciable improvement was obtained by trying a more complicated trial function.

In Fig. 4, $f(t)/f(0)$ is plotted. Note that the t dependence is much flatter than that shown in Fig. 2 in the small-t region while behaving in a manner similar to the first case for large t. This behavior is consistent with our earlier result in that one would expect wave-function effects to be more important at small t and to cause a more rapid falloff in that region. We will consider this point in more detail in Sec. IV.

IV. PHYSICAL IMPLICATIONS

Once we have the quark-quark elastic amplitude $f(t)$, we must ask how to translate our results into predictions about observable particles. To do this, we first have to note that the impulse approximation may be adequate to deal with the scattering of two composite objects made up of quarks.

The mean free path for a quark in quark matter, assuming $\sigma_{qq}=\frac{1}{9}\sigma_{pp}\sim 4.5$ mb, is about 5×10^{-13} cm if the density of quarks in quark matter is 2×10^{38} cm^{-3} (corresponding to a meson radius of 1.4×10^{-13} cm). This matches the radius of the blob of quark matter, $1.4N^{1/3}\times10^{-13}$ cm, when N is around 3. Thus multiple scattering of quarks is irrelevant in mesons or baryons, though it may become important in nuclei.

If multiple scattering from the quark constituents in mesons and baryons can be neglected, then we may write for the elastic scattering amplitude of two hadrons just the impulse approximation result:

$$T = is\int d\mathbf{x}\,\psi_f^*(\mathbf{x}) \sum_{\alpha=1}^{N} e^{i\Delta\cdot\mathbf{x}_\alpha}[f_\alpha(t)]^{1/2}\psi_i(\mathbf{x}) \times \int d\mathbf{x}'\,\psi_{f'}^*(x') \sum_{\beta=1}^{N'} e^{i\Delta\cdot\mathbf{x}_\beta'}[f_\beta(t)]^{1/2}\psi_{i'}(\mathbf{x}'), \quad (4.1)$$

where $t=-\Delta^2$, and N, N' are the number of quarks in the two composite particles.

If as before we assume $SU(6)_W$ for the vertices and drop the indices $\alpha, \beta, \ldots$ on the quarks, this reduces to

$$T = isf(t)NN'V_{fi}(t)V_{f'i'}(t), \quad (4.2)$$

where we define the form factor $V_{fi}(t)$ by

$$V_{fi}(t) = \int d^3\mathbf{x}\,\psi_f^*(\mathbf{x})e^{i\Delta\cdot\mathbf{x}}\psi_i(\mathbf{x}). \quad (4.3)$$

Note that $V_{ii}(0)=1$ in virtue of the normalization of the wave functions.

TABLE II. Approximate solution for qq. The subscripts 0, 1, 2, refer to the input, first, and second iteration, respectively, of Eqs. (3.10) and (2.2). The columns labeled f are the $f_{qq}(t)$ divided by the input value of $f_{qq}(0)$.

$-t$ in GeV^2	$f(t)_{\text{input}}$	$f(t)_{\text{output}}$	$g(t)_0$	$g(t)_1$	$g(t)_2$
0.00	1.0	1.11	1.15	1.20	1.20
0.14	0.85	0.88	1.08	1.09	1.11
0.23	0.77	0.77	1.03	1.03	1.05
0.36	0.66	0.64	0.97	0.96	0.98
0.55	0.52	0.49	0.88	0.86	0.87
0.82	0.37	0.34	0.75	0.73	0.73
1.22	0.22	0.21	0.59	0.58	0.57
1.83	0.110	0.109	0.41	0.41	0.39
2.78	0.043	0.045	0.24	0.25	0.23
4.31	0.0135	0.0144	0.110	0.115	0.106
6.95	3.5×10^{-3}	3.5×10^{-3}	0.035	0.036	0.033
11.9	5.9×10^{-4}	6.3×10^{-4}	6.9×10^{-3}	7.1×10^{-3}	5.6×10^{-3}
22.2	5.9×10^{-5}	6.1×10^{-5}	7.1×10^{-4}	7.3×10^{-4}	5.4×10^{-4}

At $t=0$, consequently, and for elastic scattering, the additive quark model applies.[9] Away from $t=0$, some t dependence is introduced through the wave function as well as that arising from the basic quark-quark scattering described by $f(t)$. We do not know much theoretically about the quark wave functions; therefore it follows that we know little about the form factors $V(t)$. However, we can reverse our thinking and use experiment plus a theoretical calculation of $f(t)$ from the integral equation (3.10) to evaluate $V(t)$, and thus learn something about the quark wave functions. From this point of view, $V(t)$ for the nucleon is just the following:

$$V(t)=\tfrac{1}{3}[f_{pp}(t)/f_{qq}(t)]^{1/2}. \tag{4.4}$$

The resulting $V(t)$ is shown in Fig. 5.

V. CONSEQUENCES

First note that diffraction scattering (for example, meson-meson) proceeds through the diagrams shown in Fig. 6. These quark diagrams clearly show the repeated vacuum exchange in the t channel which intuitively may be expected to correspond to diffraction. The fact that we have assumed $SU(6)_W$ symmetry and have not permitted the "coupling" to change the $SU(6)_W$ quark index means that we automatically obtain $SU(6)_W$ selection rules for diffraction dissociation. These are consistent with observed data.[10]

Next, note that at $t=0$ the simple additive quark model holds, as we saw in Eq. (4.2). Thus the total cross sections are in the usual ratio 9:6:4:1 for $\sigma_{BB}:\sigma_{MB}:\sigma_{MM}:\sigma_{qq}$.

The fact that $V(t)$, shown in Fig. 5, becomes constant at large t indicates the presence of a hard core, albeit with a rather small coefficient, in the spatial wave function. The spatial extent of the wave function can be deduced from the slope of $V(t)$ at $t=0$, and this slope

FIG. 6. Contribution of $q\bar{q}$ pair intermediate states to the meson-meson total cross section.

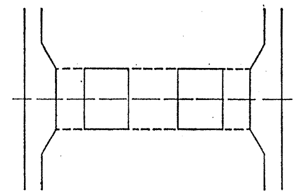

corresponds to an rms radius of about 0.8 F, which is a quite reasonable value.

Let us next turn to production processes. Qualitatively, meson production in meson-meson collisions, for example, will be described by associating $q\bar{q}$ pairs in the quark production amplitudes, keeping in mind the rule[11] of quark diagrams that a quark and an antiquark in the same meson cannot annihilate one another. One cannot, therefore, associate the quark and antiquark in a given produced $q\bar{q}$ pair. A typical acceptable diagram is shown in Fig. 7. Analogous diagrams hold for other production processes.

At the present level of complication, ratios of kinds of particles produced are simply those inherent in $SU(6)_W$. Space-time structure is not included, since with the additive quark model we do not use $q\bar{q}$ wave functions in constructing the final meson states.

Without knowledge of the wave functions, we cannot say anything definitive regarding the observed multiplicity. The average multiplicity of $q\bar{q}$ pairs is easily calculated from the model to be

$$\langle N\rangle=\tfrac{1}{2}\cosh^{-1}(\sigma_T/\sigma_e) \tag{5.1}$$

and, of course, constant. Numerically, we may expect (σ_T/σ_e) for quarks to $9(\sigma_T/\sigma_e)$ for proton-proton scattering and thus about 50. This gives $\langle N\rangle\sim2.25$, so that the average number of quarks produced is around 4.5.

Now as the energy s increases we do not produce more $q\bar{q}$ pairs but we do increase the mass of each produced meson ($q\bar{q}$ bound state). The spin of these mesons therefore also increases. Thus as s grows, we are producing $q\bar{q}$ bound states of higher and higher spin, and these decay into larger and larger numbers of low-spin $q\bar{q}$ resonances which are the final observed particles. The observed multiplicity must, then, grow, but how it grows depends on quark dynamics; it depends on the

FIG. 7. Example of a quark diagram for describing the production process $M+M\rightarrow M+M+M+M$.

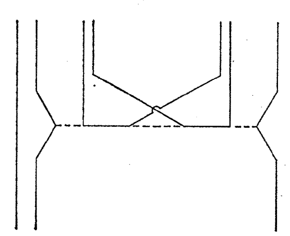

[9] H. J. Lipkin *et al.*, Phys. Rev. 152, 1375 (1967), and references therein.

[10] R. Carlitz, S. Frautschi, and G. Zweig, Phys. Rev. Letters 23, 1134 (1969).

[11] J. Rosner, Phys. Rev. Letters 22, 689 (1969); H. Harari, *ibid.* 22, 562 (1969); G. Zweig, in *Symmetries in Particle Physics*, edited by A. Zichichi (Academic, New York, 1965).

product of the amplitude to produce $q\bar{q}$ states of spin J and the amplitude for a state of spin J to decay into a given number of (relatively stable) particles.

ACKNOWLEDGMENTS

One of us (J.S.B.) would like to thank Professor G. F. Chew for his hospitality at the Lawrence Radiation Laboratory, Berkeley, where most of the numerical calculations were performed and, further, to express his gratitude to the Associated Western Universities, Inc., and the Atomic Energy Commission, whose financial support made possible this faculty orientation and training program at the Lawrence Radiation Laboratory.

PHYSICAL REVIEW D VOLUME 3, NUMBER 7 1 APRIL 1971

Implications of Local Duality in a Set of Coupled Reactions*

M. J. King and Kameshwar C. Wali
Physics Department, Syracuse University, Syracuse, New York 13210
(Received 25 September 1970)

This is an extension of the study in an earlier paper on meson-decuplet scattering to two sets of coupled reactions: (1) $PB_{10}\to PB_{10}$, $PB_{10}\to PB_8$, $PB_8\to PB_8$ and (2) $PV\to PV$, $PV\to PP$, $PP\to PP$. P and V refer to the pseudoscalar-meson octet and vector-meson nonet, respectively, while B_8 and B_{10} correspond to the octet of $J^P=\frac{1}{2}^+$ baryons and decuplet $J^P=\frac{3}{2}^+$ baryons, respectively. Some consequences of local duality are examined and compared with experiment in limited energy regions for the above reactions. The assumption that the imaginary parts of the direct-channel helicity amplitudes vanish in the forward (backward) scattering if the crossed t channel (u channel) is exotic leads to systems of equations relating resonance contributions in the direct channel. The solutions predict certain patterns of particles degenerate in mass but with different $SU(3)$, spin, and parity assignments. In particular, the inclusion of spin considerations yields the result that the particles on leading trajectories must be accompanied by daughters with prescribed ratios of coupling constants between the parent and daughter states. We discuss the link between our results and those which follow from a complementary description in terms of Regge residues.

I. INTRODUCTION

Combining crossing, $SU(3)$ symmetry, and duality, several authors have predicted certain exchange-degeneracy patterns for hadronic trajectories.[1,2] These considerations have presented a new approach to the classification of hadrons. In this approach it is assumed that the imaginary part of the resonant scattering amplitude is expressible, at high energies, in terms of Regge trajectories in the crossed channels. Hence if a particular scattering amplitude is characterized by internal quantum numbers for which no resonances exist, the Regge trajectories in the crossed channels must exhibit exchange degeneracy so that the corresponding imaginary parts cancel.

A complementary description of the resonant part of the scattering amplitude exists in terms of direct-channel resonances. One can assume, therefore, that there is a region of s and small t on the one hand, and a region of s and small u on the other, within which the imaginary part can be calculated in two alternative ways: in terms of direct-channel resonances *or* in terms of Regge trajectories of the crossed channels.[3] If we select the s-channel reactions so that their t or u channels are characterized by exotic quantum numbers, the imaginary parts due to s-channel resonances must add up to zero. We have investigated the consequences of this assumption in a local energy region (local duality) in the case of the following set of coupled reactions:

(1) $\quad PB_{10}\to PB_{10},\ PB_{10}\to PB_8,\ PB_8\to PB_8,$

(2) $\quad PV\to PV,\quad PV\to PP,\quad PP\to PP,$

where P represents the pseudoscalar meson octet, B_{10} represents the decuplet of $J^P=\frac{3}{2}^+$ baryons, B_8 represents the octet of $J^P=\frac{1}{2}^+$ baryons, and V represents the nonet of vector mesons.

In each of these reactions, we consider a set of direct-channel resonances degenerate in mass but with different spins and parities, and examine the constraints on their coupling constants. The choice of such a system of resonances degenerate in mass is, in part, motivated by the experimental evidence in certain energy regions for a number of πN (and $\pi\pi$) resonances approximately equal in mass although differing in spin, isospin, and parity. Further, there is evidence that they are coupled to $\pi\Delta$ (and $\pi\rho$) systems. $SU(3)$ symmetry would then require the consideration of reactions (1) and (2). The assumption, in part, is also motivated by the properties of Veneziano-type models[4] which attempt to incor-

* Work supported by the U. S. Atomic Energy Commission.
[1] R. H. Capps, Phys. Rev. Letters **22**, 215 (1969); J. Mandula *et al.*, *ibid.* **22**, 1147 (1969); V. Barger and C. Michael, Phys. Rev. **186**, 1592 (1969).
[2] L. K. Chavda and R. H. Capps, Phys. Rev. D **1**, 1845 (1970).
[3] J. Mandula, J. Weyers, and G. Zweig, Phys. Rev. Letters **23**, 627 (1969).
[4] G. Veneziano, Nuovo Cimento **57A**, 190 (1968).